Kinetic Characterization of the Catalytic Domain of *Dictyostelium discoideum* Myosin[†]

Sally K. A. Woodward,[‡] Michael A. Geeves,[§] and Dietmar J. Manstein*,[‡]

National Institute for Medical Research, The Ridgeway, Mill Hill, London NW7 1AA, U.K., and Max-Planck-Institut für Molekulare Physiologie, Rheinlanddamm 201, D-44139 Dortmund, Germany

Received July 12, 1995; Revised Manuscript Received October 9, 1995[⊗]

ABSTRACT: The myosin head consists of a globular motor or catalytic domain that contains both the catalytic and actin binding sites, and a neck region which consists of a 8.5 nm α-helix that emerges from the globular part of the heavy chain and is stabilized by the binding of the essential and regulatory light chains. High levels of M754, a recombinant polyhistidine-tagged catalytic domain-like fragment of myosin II, were produced in *Dictyostelium discoideum* and purified using a rapid extraction protocol and metal chelate chromatography. Approximately 1.2 mg of homogeneous, functional protein was obtained per gram of cells. Kinetic analysis of M754 showed that the recombinant protein still has all the typical properties of a myosin ATPase. However, the removal of the light chain domain does have a pronounced effect on enzymatic activity. Nucleotide on-rates are 7−16-fold slower for M754 than for a myosin head fragment that includes the neck region. In contrast, the rate of ATP binding and dissociating the actin-bound catalytic domain is 10-fold increased. Overall the results indicate that the truncation of the heavy chain affects the nucleotide binding site and the communication between the nucleotide and actin binding sites. Furthermore, it seems that the nucleotide site of M754 is not fully formed but binding to actin or ATP stabilizes the structure in general and the nucleotide binding site in particular.

Members of the myosin family interact with actin filaments and adenosine 5′-triphosphate (ATP)[1] to produce mechanical force and displacement. This interaction is the basis of such diverse phenomena as muscle contraction, cytoplasmic streaming in plants, amoeboid movement, and cytokinesis. The exact mechanism by which myosin transduces the chemical energy derived from ATP hydrolysis into force and displacement is still not fully understood. However, essential features of the actomyosin ATPase reaction were deduced from transient kinetic studies using actin filaments and myosin subfragment 1 (S1) in solution and by comparing the results with those obtained from mechanical, optical, and structural measurements on rate processes in intact muscle fibers (Goldman et al., 1982; Huxley et al., 1983; Lombardi et al., 1995). The model of the mechanochemical ATPase cycle that emerged from these studies (Lymn & Taylor, 1971; Taylor, 1979; Trentham et al., 1976; Geeves et al., 1984; Rayment et al., 1993b) is generally in good agreement with the recent progress that was made using structural approaches (Rayment et al., 1993a,b; Schröder et al., 1993; Fisher et al., 1995b) and *in vitro* functional assays (Uyeda et al., 1991; Finer et al., 1994). Further insights into molecular motor function can be obtained by combining the approaches mentioned above with molecular genetics. The lower eukaryote *D. discoideum* has emerged as a powerful system for this purpose.

Previously we carried out a kinetic characterization of the *D. discoideum* myosin head fragment (MHF), using rapid reaction and equilibrium measurements (Ritchie et al., 1993). MHF, a recombinant protein, equivalent in size to rabbit S1, binds to actin with the same affinity as rabbit skeletal S1. The ATP-induced isomerization of acto−MHF is 10-fold slower than for acto−S1, and the rate of binding of ATP to MHF, the subsequent cleavage step, and the rate of mantADP binding are significantly slower than for S1. MantADP dissociates 5-fold faster from MHF than from rabbit S1, which together with the slower association rate constant indicates a weaker association binding constant. Overall, however, the interaction of MHF with nucleotide and actin appears to follow the same basic mechanism as for S1 from rabbit fast muscle myosin and other muscle myosins (Marston & Taylor, 1980). This provides the basis for the dissection of myosin motor function using genetically altered myosin head fragments.

Here we extend this integrated molecular genetic and kinetic approach to study a recombinant, catalytic domain-like fragment of conventional *D. discoideum* myosin (DCD). The catalytic domain corresponds to the globular portion of the myosin head that contains ATP and actin binding sites but lacks the light chain domain (LCD). M754, a recombinant protein that corresponds to the DCD, was generated

[†] Supported by the Medical Research Council and the Max-Planck-Society.

* Author to whom correspondence should be addressed.
[‡] National Institute for Medical Research.
[§] Max-Planck-Institut für Molekulare Physiologie.

[⊗] Abstract published in *Advance ACS Abstracts,* November 15, 1995.

[1] Abbreviations: ADP, adenosine 5′-diphosphate; ATP, adenosine 5′-triphosphate; *D.*, *Dictyostelium*; DCD, catalytic domain of *D. discoideum* myosin; Ddp2, *D. discoideum* plasmid; DTT, 1,4-dithiothreitol; EDTA, ethylenediaminetetraacetic acid; EGTA, ethylene glycol bis(β-aminoethyl ether)-*N,N,N′,N′*-tetraacetic acid; kb, kilobase(s); K_D, dissociation constant; LCD, light chain domain; mantADP, 2′(3′)-*O*-(*N*-methylanthraniloyl)adenosine 5′-diphosphate; M754, recombinant protein corresponding to the DCD; MHC, myosin heavy chain; *mhcA*, gene encoding MHC; MHF, S1-like fragment of *D. discoideum* myosin; NADH, nicotinamide adenine dinucleotide; NTA, nitrilotriacetic acid; ORF, open reading frame; PCR, polymerase chain reaction; PEP, phosphoenolpyruvate; PK, pyruvate kinase; PMSF, phenylmethanesulfonyl fluoride; S1, subfragment 1 of myosin; SDS, sodium dodecyl sulfate; TLCK, *N*-tosyl-L-lysine chloromethyl ketone.

0006-2960/95/0434-16056$09.00/0

using PCR-directed mutagenesis which results in the truncation of the *D. discoideum mhc*A gene at a position corresponding to Ile-754. This site of truncation is equivalent to residue Leu-775 in chicken skeletal muscle myosin. A similar recombinant fragment of *D. discoideum* myosin, truncated at Glu-759 (Asp-780 in chicken skeletal muscle myosin), was shown to function as a molecular motor *in vitro* (Itakura et al., 1993), and the structures of the MgADP−beryllium fluoride, MgADP−aluminum fluoride, and Mg(II)−pyrophosphate complexes of this catalytic domain fragment were solved recently (Fisher et al., 1995a,b; Smith & Rayment, 1995).

The missing LCD, which is sometimes also referred to as "neck domain" or "regulatory domain", is thought to have a dual function. Enzymatic and functional studies have been used to demonstrate that this region has a modulating effect on myosin motor activity (Taylor, 1979; Sellers, 1985; Lowey et al., 1993), and structural studies suggest that the complex of the extended heavy chain α-helix and the essential and regulatory light chains forms a rigid complex of approximately 10 nm length that may function as a "lever arm" to amplify the conformational changes in the nucleotide and actin binding sties of the catalytic domain (Rayment et al., 1993b; Xie et al., 1994). Disruptions of the structural integrity of the LCD, by removal of light chains or shortening of the domain by removing the binding site for one or both of the light chains, result in a proportional reduction in the velocity of actin filaments, as measured in an *in vitro* motility assay, while the steady-state actin-activated ATPase is not significantly decreased or even increased (Lowey et al., 1993; Uyeda & Spudich, 1993; Itakura et al., 1993).

In the experiments presented here, we describe our efforts to improve the production of active myosin motor domains in *D. discoideum* and report the kinetic characterization of M754, a catalytic domain-like fragment. M754 was produced using a new extrachromosomal expression vector for the production of His-tagged proteins (Manstein et al., 1995). The truncated protein was purified by recruitment into a rigor-like complex with actin and selective solubilization upon addition of MgATP, followed by Ni^{2+}−nitrilotriacetic acid (NTA) affinity chromatography. Approximately 1.2 mg of active M754 was purified per gram of cells. The results of the kinetic characteriztion of the interaction of the truncated myosin with nucleotides and actin demonstrate that the removal of the light chain binding region has a pronounced effect on the nucleotide binding site. Specifically, the tightness of nucleotide binding and the rates for nucleotide dissociation are altered.

MATERIALS AND METHODS

Plasmid Construction and Mutagenesis. General cloning techniques were performed as described by Sambrook et al. (1989). Enzymes were from Boehringer Mannheim and New England Biolabs. *Escherichia coli* strains XL1 Blue (*rec*A1, *end*A1, gyrA96, *thi*-1, *hsdR*17, *sup*E44, *rel*A1, *lac*, [F′ *pro*AB, *lacI*^{q} ZΔM15, Tn10(tet^r)]) (Stratagene) and JM103 (*end*A1, *hsdR*, *supE*, *sbcBC*, *thi*-1, *strA*, Δ(*lac-pro*), [F′ *traD*36, *lacI*^{q}ZΔ*M*15, *proAB*]) (Yanisch-Perron et al., 1985) were used for DNA manipulations.

The plasmid pSW29, containing the catalytic domain of the *D. discoideum mhc*A gene linked to an affinity tag consisting of eight His residues, and under the control of the *actin*15 promoter, was created as follows: PCR-directed mutagenesis was carried out to create a unique *Xba*I site as described by Perrin and Gilliland (1990). This permitted the isolation of a fragment of the *mhcA* gene encoding amino acids 1−754. Four oligonucleotides were used for the PCR reactions: two mutagenic primers and two nonmutagenic oligonucleotides that prime from either side to the mutation, outside of unique *Bgl*II and *Nco*I restriction sites in the gene. The mutagenic primer pair used to create the *Xba*I restriction site 2330 bp from the origin of the gene was $^{5'}$GGTCAATT-AGCTCGTATTCTAGAAGCTCGTGAACAACG$^{3'}$ and $^{5'}$CGTTGTTCACGAGCTTCTAGAATACGAGC-TAATTGACC$^{3'}$. The resulting PCR product was digested with *Bgl*II/*Nco*I to give a 643 base pair fragment. This fragment was subcloned into the *Bgl*II and *Nco*I sites of pMyΔ to create pSW10. The plasmic pMyΔ, which contains the *D. discoideum mhc*A gene from the *Bst*XI site at position 1791 to the end of the gene, was constructed by subcloning the *Bst*XI (blunt)−*Kpn*I fragment of pMyD (De Lozanne & Spudich, 1987) into the *Xba*I (blunt)−*Kpn*I sites of pTZ18R. The fragment containing the mutation was verified by DNA sequencing. Next, a 2.15 kb *Sal*I−*Bgl*II fragment from pSW6, containing the N-terminal part of the gene, was subcloned into the *Sal*I and *Bgl*II sites of pSW10. The resulting plasmid, pSW17, contained the entire *mhc*A gene under control of the *actin*15 promoter, with the *Xba*I restriction site created at 2330 bp. To construct the C-terminally His-tagged M754, pSW17 was digested with *Kpn*I/*Xba*I, and the 2.3 kb fragment was ligated into the *D. discoideum* expression vector pDXA-3H (Manstein et al., 1995). pDXA-3H carries the origin of replication of the *D. discoideum* high copy number plasmid Ddp2 (Leiting et al., 1990; Chang et al., 1990) and sequences that facilitate the addition of a His-tag to the C-terminus of any protein. The resulting plasmid, pSW29, was transformed into AX3-ORF$^+$ cells which have several copies of the *ORF* gene integrated in their genome (Manstein et al., 1995). The *ORF* gene is known to be essential in *trans* for the replication of plasmids carrying the Ddp2 origin (Slade et al., 1990; Leiting et al., 1990). Transformations were carried out by electroporation as described by Egelhoff and co-workers (Egelhoff et al., 1991). Transformation efficiencies of ~5 × 10^4 were observed. The relative amounts of M754 produced by individual transformants were estimated from Coomassie blue-stained SDS−polyacrylamide gels after selective enrichment of functional myosins by recruitment into a complex with actin and solubilization by addition of MgATP (Manstein & Hunt, 1995). Transformants showing the highest level of expression were used for further studies.

Purification of M754. Cells from the cell line HDM-29-3, expressing M754, were grown in 5 L flasks containing 2.5 L of DD-Broth 20 [20 g/L protease peptone (Oxoid), 7 g/L yeast extract (Oxoid), 8 g/L glucose, 0.35 g of KH_2PO_4, and 0.47 g/L $Na_2HPO_4 \cdot 12H_2O$, pH 6.5]. The flasks were incubated on a gyratory shaker at 200 rpm and 22 °C. Cells were harvested at a density of (6−8) × 10^6 mL^{-1} by centrifugation for 7 min at 2700 rpm in a Beckman J-6 centrifuge and washed once in phosphate-buffered saline. The wet weight of the resulting cell pellet was determined. Typically, 50 g was obtained from a 15 L shaking culture. The cells were resuspended in 200 mL of lysis buffer [50 mM Tris·HCl, pH 8.0, 2 mM EDTA, 0.2 mM EGTA, 1 mM dithiothreitol (DTT), 5 mM benzamidine, 40 μg/mL *N*-tosyl-

L-lysine chloromethyl ketone (TLCK), and 40 μg/mL phenylmethanesulfonyl fluoride (PMSF)]. Cell lysis was induced by the addition of 100 mL of lysis buffer containing 1% Triton X-100, 15 μg/mL RNase A, and 100 units of alkaline phosphatase (Boehringer Mannheim). The lysate was incubated on ice for 1 h. Upon centrifugation (230000g, 1 h), M754 remained in the pellet. The pellet was washed in 100 mL of HKM buffer (50 mM HEPES, pH 7.3, 30 mM potassium acetate, 10 mM $MgSO_4$, 7 mM β-mercaptoethanol, 5 mM benzamidine, and 40 μg/mL PMSF) and centrifuged for 45 min at 230000g. M754 was released into the supernatant by extraction of the resulting pellet with 80 mL of HKM buffer containing 10 mM ATP. After centrifugation (500000g, 45 min), the supernatant was applied with a peristaltic pump to a Ni^{2+}−NTA affinity column (Qiagen). The flow-rate was adjusted to approximately 3 mL min^{-1}. After loading was completed, the column was connected to a Waters 650M chromatography system. The column was washed briefly in low salt buffer (50 mM HEPES, pH 7.3, 30 mM potassium acetate, and 3 mM benzamidine), high salt buffer (same as low salt buffer, but with 300 mM potassium acetate), and low salt buffer containing 50 mM imidazole. M754 was eluted using a linear gradient of low salt buffer and imidazole buffer (0.5 M imidazole, pH 7.3, 3 mM benzamidine), starting with 10% imidazole buffer and reaching 100% after 15 min. The flow rate was 3 mL min^{-1}, and 3 mL fractions were collected. The absorbance at 280 nm was monitored. SDS−polyacrylamide gels were run to check the purity of the eluted protein (Figure 1). M754 was concentrated using a Centriprep 30 device (Amicon) and dialyzed against the appropriate buffer for stopped-flow experiments.

Stopped-Flow and Fluorescence Titrations. Experiments were carried out in SF-buffer (25 mM HEPES, 0.1 M KCl, and 5 mM $MgCl_2$, pH 7.0) at 20 °C, unless otherwise stated. In stopped-flow experiments, concentrations after mixing are quoted.

Fluorescence stopped-flow experiments were carried out on a Hi-tech Scientific SF-61MX spectrophotometer equipped with a 100 W mercury lamp. Excitation light was obtained using a monochromator, and emission was through an appropriate band-pass or cutoff filter. For tryptophan fluorescence, excitation was at 290 nm, with emission through a WG 320 cutoff filter. Mant fluorescence was excited at 366 nm with emission through a Wratten 47B filter. For light-scattering measurements, the incident light at 330 nm was monitored through a WG 320 cutoff filter, and for pyrene fluorescence, excitation was at 365 nm with emission through a 390 nm cutoff filter. Data were stored and analyzed using software provided by Hi-tech.

Fluorescence titrations were carried out on an SLM 8000S spectrofluorometer. A working volume of 1 mL in a 1 cm path length cuvette was used. Pyrene fluorescence was excited at 365 nm with emission at 407 nm, through monochromators.

Actin Activation. Actin activation (at actin concentrations <15 μM) was measured on a Beckman DU70 spectrophotometer using a linked enzyme assay system. Steady-state ATPase rates were measured in a solution containing 15 mM HEPES, pH 7.0, 4 mM $MgCl_2$, 1 mM ATP, 1 mM DTT, 0.17 mg/mL PEP, 0.17 mg/mL NADH, 33 mg/mL LDH, and 29 mg/mL PK. The basal ATPase rate of M754 in the absence of actin was measured, followed by the steady-state

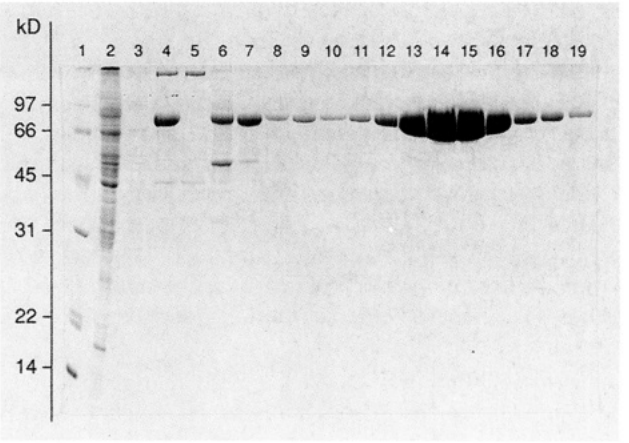

FIGURE 1: Purification of M754. The proteins present in pertinent fractions of the purification procedure were resolved by 12% SDS−PAGE and visualized by Coomassie Blue staining (7 μL of each fraction was loaded per lane). Molecular mass markers (lane 1). Cells grown to a density of 7 × 10^6/mL were washed in phosphate-buffered saline, lysed, and depleted of ATP (lane 2). Upon centrifugation, the recombinant protein remained in the pellet and not in the supernatant (lane 3). Extraction of the pellet with 10 mM MgATP released M754 into the supernatant (lane 4). The high-speed supernatant was applied to a Ni^{2+}−NTA column (1.5 × 11 cm): flow through (lane 5); wash with 50 mM imidazole (lanes 6, 7); homogeneous M754 was eluted using a linear gradient from 50 to 500 mM imidazole (lanes 8−19).

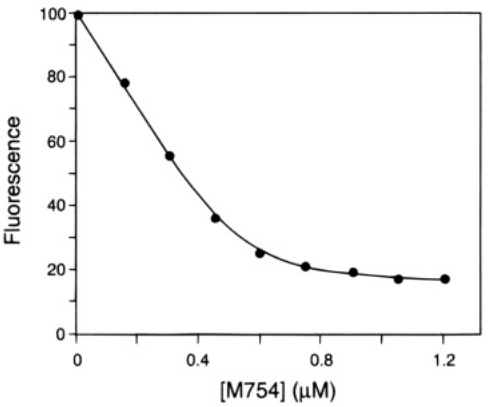

FIGURE 2: Fluorescence titration of 0.5 μM pyrene-actin with M754. The dissociation constant was determined as described by Geeves and Jeffries (1988), and a value of 0.04 μM was obtained. Conditions: 25 mM HEPES, 100 mM KCl, 5 mM $MgCl_2$, pH 7.0, 20 °C. 0.5 μM phalloidin was used to stabilize the F-actin.

ATPase upon the addition of actin. Typical working volumes of 600−800 μL were used. Additionally, actin-activated (at actin concentrations >15 μM) and high-salt Ca^{2+}-activated ATPase activities were measured as described by White (1982).

Proteins and Reagents. Rabbit actin was purified by the method of Lehrer and Kerwar (1972). Its molar concentration was determined using an extinction coefficient of $\epsilon^{1\%}_{280nm}$ = 11.08 cm^{-1} and a molecular weight of 42 000 (West et al., 1967). The preparation of pyrene-labeled actin was as previously described (Criddle et al., 1985). In determining the concentration of pyrene-actin, a correction was made for the absorbance of the label at 280 nm [A_{280}(pyr) = 1.06 × A_{344} (Criddle et al., 1985)].

2′(3′)-*O*-(*N*-Methylanthraniloyl) derivatives of ATP and ADP (mantATP, mantADP) were prepared by reaction with *N*-methylisatoic anhydride (Molecular Probes) as described by Hiratsuka (1983), except that after reaction they were

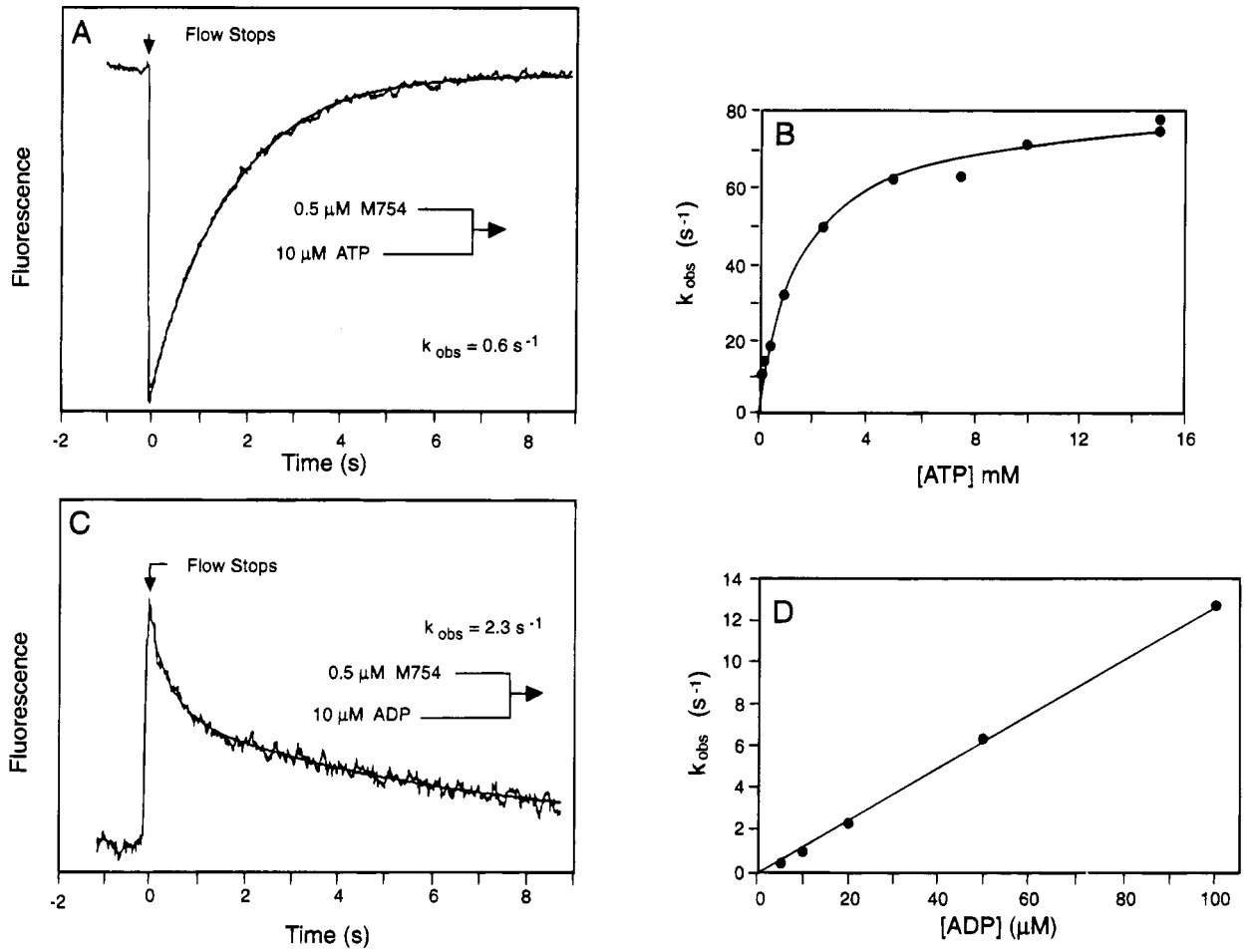

FIGURE 3: Binding of nucleotides to M754. (A) Stopped-flow record of the binding of ATP to M754. 0.5 μM M754 was rapidly mixed with 10 μM ATP, monitoring tryptophan fluorescence. The solid line is the best fit of the data to a single exponential. $k_{obs} = 0.6\ s^{-1}$. (B) Dependence of the rate of the observed processes on ATP concentration. The data were fitted to a hyperbolic function, with a maximum value of 80 s^{-1}. The observed rate was linear over the range 5−100 μM ATP, with a second-order binding constant of $5.7 \times 10^4\ M^{-1}\ s^{-1}$. (C) Stopped-flow record obtained upon mixing 0.5 μM M754 with 10 μM ADP, monitoring tryptophan fluorescence. The solid line is the best fit of the data to a single exponential with a sloping base line. $k_{obs} = 2.3\ s^{-1}$. (D) Dependence of the rate of the observed processes on ADP concentration. The data were fitted to a straight line, the slope of which gave a second-order binding constant of $1.25 \times 10^5\ M^{-1}\ s^{-1}$.

purified on a DEAE-cellulose column as described in Woodward et al. (1991).

RESULTS

Protein Purification. The purification of M754 is shown in Figure 1. Following Ni^{2+}−NTA chromatography, the protein was >95% pure as estimated from the Coomassie Blue stained polyacrylamide gel (Figure 1, lanes 8−19). Typically, 60 mg of pure M754 was obtained from 50 g of cells.

M754 consists of 774 amino acids due to the substitution of residue Asn-2 with the pentapeptide Asp-Gly-Thr-Glu-Asp and a 16 amino acid C-terminal extension (Leu-Gly-Ser-Thr-Arg-Asp-Ala-Leu-His-His-His-His-His-His-His-His) that includes the Ni^{2+}-ion affinity tag. The molecular weight of M754 was calculated as 88 100, and a molar extinction coefficient of 60 000 at 280 nm was determined.

Equilibrium Binding of M754 to Actin. The quenching of fluorescence that occurs upon binding of myosin to pyrene-labeled actin (Kouyama & Mihashi, 1981; Geeves & Jeffries, 1988) was used to monitor the interaction of M754 with actin. A titration of 0.5 μM pyr-actin with M754 at low ionic strength (20 mM HEPES, 2 mM $MgCl_2$, pH 7.0) shows that M754 binds to pyr-actin and quenches the fluorescence by 80%. Under the conditions of this titration, the concentration of pyr-actin is much greater than the equilibrium dissociation constant, and saturation of actin occurs at stoichiometric M754 concentration.

The affinity of M754 for actin was determined in 0.1 M KCl by titration of 0.5 μM pyr-actin with 0−1.2 μM M754 (Figure 2). The quenching of pyrene fluorescence was again 80%. The dissociation constant was determined as described earlier (Geeves & Jeffries, 1988), and a value of 0.04 μM was obtained. This K_D is similar to the values obtained for MHF (0.07 μM) and rabbit S1 (0.07 μM) (Ritchie et al., 1993).

Steady-State Rate of ATP Hydrolysis by M754. The ability of actin to activate the hydrolysis of ATP by M754 was measured under low salt conditions. The basal Mg^{2+}-ATPase activity of M754 was 0.04 s^{-1}, and the rate of ATP hydrolysis increased almost linearly on addition of actin. A rate of 4.8 s^{-1} was measured in the presence of 40 μM actin and 2 mM Mg^{2+}-ATP. In the absence of actin and at high ionic strength, M754 displayed an ATPase activity of 8.7 s^{-1} in the presence of Ca^{2+}.

Table 1: Summary of Rate Constants for the Interaction of Nucleotides with Rabbit S1 and *D. discoideum* MHF and M754[a]

$$M + ATP \underset{k_{-1}}{\overset{k_{+1}}{\rightleftharpoons}} M{\cdot}ATP \underset{k_{-2}}{\overset{k_{+2}}{\rightleftharpoons}} M^{*}{\cdot}ATP \underset{k_{-3}}{\overset{k_{+3}}{\rightleftharpoons}}$$

$$M{\cdot}ADP{\cdot}P_i \underset{k_{-4}}{\overset{k_{+4}}{\rightleftharpoons}} M{\cdot}ADP \underset{k_{-5}}{\overset{k_{+5}}{\rightleftharpoons}} M + ADP$$

nucleotide	rate constant	S1	MHF	M754
ATP	$K_1 \times k_{+2}$ (M^{-1} s^{-1})	1.9×10^6	9.4×10^5	5.7×10^4
	$k_{+3} + k_{-3}$ (s^{-1})	131	24	80
mantATP	$K_1 \times k_{+2}$ (M^{-1} s^{-1})	3.2×10^6	7.0×10^5	1.0×10^5
ADP	k_{-5} (M^{-1} s^{-1})	2×10^6	nd	1.25×10^5
	k_{+5} (s^{-1})	2	nd	0.06
	K_5 (μM)	1	30	0.4
mantADP	k_{-5} (M^{-1} s^{-1})	2.9×10^6	9×10^5	1.25×10^5
	k_{+5} (s^{-1})	0.22	1.5	0.02
ATP	k_{cat} (s^{-1})	0.05	0.04	0.04

[a] $K_1 \times k_{-2}$ and k_{-5} = observed second-order rate constants of nucleotide binding to myosin subfragments, where the observed rate of binding was proportional to nucleotide concentration. $k_{+3} + k_{-3}$ = limiting rate constant of protein fluorescence signal at high concentrations of nucleotide. k_{+5} = observed first-order rate constant from displacement experiments. Data for rabbit S1 and MHF are from Ritchie et al. (1993).

ATP and MantATP Binding to M754. The binding of ATP to the catalytic domain was monitored by observing the intrinsic protein fluorescence following addition of excess ATP to M754. A 9% increase in fluorescence was observed, and the observed processes could be fitted to a single exponential (Figure 3A). The observed rate constant was linearly dependent on the concentration of ATP up to 100 μM, with a second-order binding constant of 5.7×10^4 M^{-1} s^{-1}. At higher ATP concentrations, up to a maximum of 15 mM, this dependence could be fitted to a hyperbola (Figure 3B), and a plateau value of 80 s^{-1} was determined. The observed rate constant also reaches a maximum for rabbit S1 and MHF, although at significantly different values (Table 1). In fact, if ATP binding is irreversible (as expected by analogy with S1), a hyperbolic function is not expected. The good fit to a hyperbola is partly due to the small change in fluorescence observed on ATP binding for the *D. discoideum* proteins compared to rabbit S1. As the hyperbolic fit probably has no real meaning, only the second-order rate constants at low ATP concentrations and the plateau values are quoted in Table 1. For S1, the plateau has been assigned to the rate constant for the ATP cleavage step, and the second-order rate constant to K_1k_{+2}. We assume the same assignment holds for MHF and M754.

The binding of mantATP to the catalytic domain was also monitored. An enhancement of fluorescence of approximately 2.2-fold was observed upon binding substoichiometric concentrations of mantATP, similar to that seen with MHF and rabbit S1. The observed processes with excess mantATP were best fitted to a double exponential, the fast phase of which increased linearly with mantATP concentration over the range 5−50 μM with a second-order binding constant of 1×10^5 M^{-1} s^{-1}. The slow phase was independent of mantATP concentration and was approximately 0.09 s^{-1}.

ADP and MantADP Binding to M754. Binding of ADP to M754 causes a quenching of the intrinsic protein fluorescence that can be used to measure the rate of ADP binding. In contrast, addition of ADP to MHF does not produce a change in protein fluorescence. The observed rate of binding was linearly dependent on the concentration of ADP over the range 5−100 μM. However, this was not a clean exponential process and was followed by a slow, further decrease of fluorescence (Figure 3C) which was identified as photobleaching. The second-order binding constant of ADP to M754 was 1.25×10^5 M^{-1} s^{-1} (Figure 3D).

We repeated these experiments using excess mantADP in place of ADP. An increase in fluorescence was observed that was best fitted by a double exponential. The fast phase increased linearly with mantADP concentration over the observed range of 5−50 μM. A second-order binding constant of 1.25×10^5 M^{-1} s^{-1} was calculated. The slow phase remained constant over this concentration range at approximately 1 s^{-1}.

ADP and MantADP Dissociation from M754. The rate of ADP dissociation from M754 was monitored by observing the intrinsic tryptophan fluorescence in a displacement experiment. A solution containing 0.5 μM M754 and 20 μM ADP was rapidly mixed with 100 μM ATP. An enhancement of tryptophan fluorescence was observed which could be fitted to a single exponential with a rate constant of 0.06 s^{-1}. The experiment was repeated using mantADP monitoring the mant fluorescence. An exponential decrease in fluorescence occurred with a rate constant of 0.02 s^{-1}.

ATP-Induced Dissociation of Acto·M754. The binding of ATP to acto·M754 was monitored by observing the decrease in light scattering as acto·M754 dissociates following ATP binding; 0.2 μM acto·M754 was rapidly mixed with increasing concentrations of ATP. The resulting exponential decrease in light scattering (Figure 4A) was linearly dependent on ATP concentration up to 100 μM, with a second-order binding constant of 1.5×10^6 M^{-1} s^{-1} (Table 2). There was evidence of biphasicity in the observed processes when measured over a longer time scale, in the form of a slow phase with a rate constant of approximately 3 s^{-1} that was independent of ATP concentration. At higher concentrations of ATP, the rate constant of the fast phase was no longer linearly dependent on ATP concentration, but could be fitted to a hyperbola (Figure 4B). This was analyzed in terms of a model used previously for acto·S1 and acto·MHF:

$$A{\cdot}M + ATP \overset{K_1}{\rightleftharpoons} A{\cdot}M{\cdot}ATP \overset{k_{+2}}{\rightleftharpoons} A + M{\cdot}ATP$$

in which A and M represent actin and M754, respectively. The first step is a rapid equilibrium between A·M and A·M·ATP defined by the equilibrium constant K_1, while the second step is the isomerization of the complex which limits the rate of dissociation of actin from the complex. For this model (Millar & Geeves, 1983), the dependence of the observed rate of ATP-induced dissociation of acto·M754 is defined by

$$k_{obs} = K_1k_{+2}[ATP]/(1 + K_1[ATP])$$

Although the data fit a hyperbola reasonably well, the errors on the rate constants above 400 s^{-1} are large. In addition, the amplitudes of the reaction decrease at higher ATP concentrations more than predicted from the dead times of the stopped-flow apparatus. Thus, K_1 and k_{+2} were estimated as $\leq$1000 M^{-1} and $\geq$800 s^{-1}, respectively. The

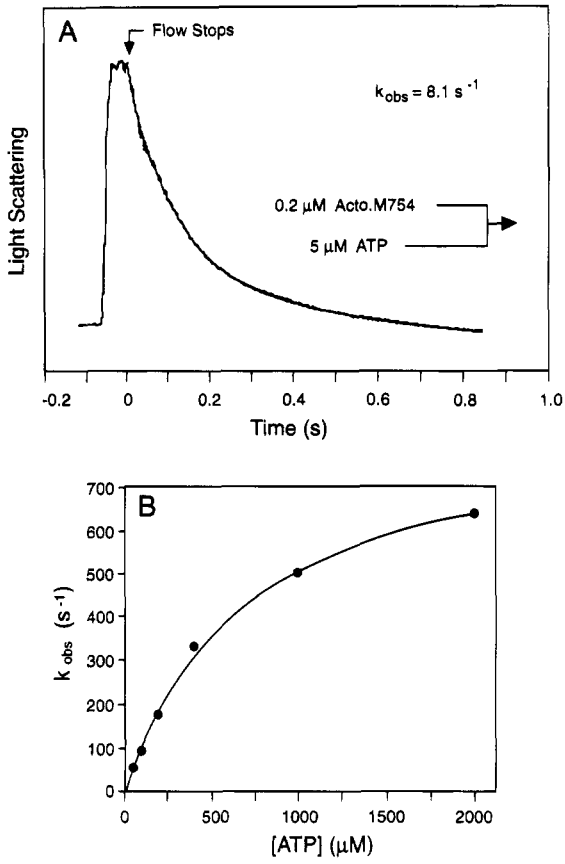

FIGURE 4: Binding of ATP to acto•M754. (A) Stopped-flow record observed on mixing 0.5 μM acto•M754 with 10 μM ATP. Light scattering was monitored. The solid line is the best fit to a single exponential. k_{obs} = 8.1 s^{-1}. (B) Determination of the maximal rate of acto•M754 dissociation. 0.5 μM acto•M754 was mixed with increasing concentrations of ATP. Light scattering was monitored. The observed rate constant was linear over the range 5−60 μM ATP, with a second-order binding constant of 1.5 × 10^6 M^{-1} s^{-1}. The maximum rate constant of the dissociation of acto•M754 by ATP was 360 s^{-1}.

Table 2: Summary of Rate Constants for the Interaction of Nucleotides with Acto•S1, Acto•MHF, and Acto•M754[a]

$$A + M \overset{K_D}{\rightleftharpoons} A{\cdot}M + ATP \overset{K_1}{\rightleftharpoons} A{\cdot}M{\cdot}ATP \xrightarrow{k_{+2}} A + M{\cdot}ATP$$

$$A{\cdot}M\ ADP \overset{K_d}{\rightleftharpoons} A{\cdot}M + ADP$$

nucleotide	rate constant	acto•S1	acto•MHF	acto•M754
ATP	$K_1 \times k_{+2}$ (M^{-1} s^{-1})	2.5 × 10^6	1.4 × 10^5	1.5 × 10^6
	K_1 (M^{-1})	500[b]	330	≤1500
	k_{+2} (s^{-1})	5000[b]	450	≥800
ADP	K_d (μM)	117	94	0.4
	k_{off} (s^{-1})	≥500[c]	nd	2.3
mantADP	k_{off} (s^{-1})	400; 2[d]	nd	5; 1
	K_D (μM)	0.07	0.07	0.04

[a] $K_1 \times k_2$ = observed second-order rate constant of nucleotide binding to actomyosin subfragments at nucleotide concentrations where the observed rate constant was proportional to nucleotide concentration. Data for S1 and MHF are from Ritchie et al. (1993). As predicted by [b] Millar and Geeves (1983), [c] Siemankowski and White (1984), and [d] Woodward et al. (1991).

second-order rate constant of ATP binding to acto•M754 (K_1k_{+2}) was determined as 1.5 × 10^6 M^{-1} s^{-1}.

Affinity of ADP for Acto•M754. On mixing a solution of 0.2 μM acto•M754 and 20 μM ADP with 1 mM ATP, we observed a single-exponential decrease in light scattering with a rate constant of 2.3 s^{-1}, independent of the ATP concentration. In the absence of ADP, the equivalent rate was 56.1 s^{-1}. This result suggests that ADP binds tightly to acto•M754 with a dissociation rate constant of 2.3 s^{-1}. Mixing ATP with acto•M754 in the presence of substoichiometric concentrations of ADP gave a biphasic dissociation reaction: a fast phase as ATP bound to ADP-free acto•M754 with the same observed rate constant as in the absence of ADP (55.7 s^{-1}), and a slow phase with an observed rate constant of 2.3 s^{-1} (Figure 5). Measuring the relative amplitudes of the fast and slow phases of acto•M754 dissociation gives an estimate of the relative concentrations of acto•M754 and acto•M754•ADP at equilibrium. Repeating the measurement at different ADP concentrations allowed the dissociation binding constant of ADP for acto•M754 to be calculated as 0.3−0.6 μM. A binding constant of this size is difficult to estimate because of the presence of contaminating ADP in the actin solution.

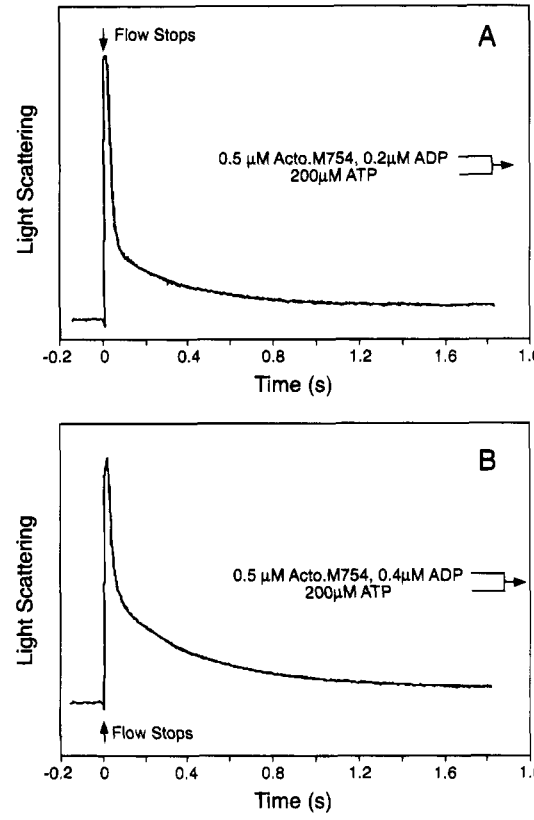

FIGURE 5: Equilibrium binding constant of ADP to acto•M754. (A) 0.5 μM acto•M754 and 0.2 μM ADP were rapidly mixed with 200 μM ATP. Light scattering was monitored. The resulting processes were fitted by a double exponential. k_{obs} = 55.7 and 2.6 s^{-1}. The ratio of the relative amplitudes of the fast and the slow phases was 3:1. (B) As (A) but using 0.4 μM ADP. The observed processes were fitted by a double exponential with rate constants of 49.4 and 2.6 s^{-1}. The ratio of the relative amplitudes of these phases was 1.3:1.

The tight binding of ADP to acto•M754 suggests that ADP will compete effectively with ATP for the actomyosin binding site. To test this, the ATP-induced dissociation of acto•M754 was examined by premixing the ATP with various concentrations of ADP. The results of an experiment where 0.25 μM acto•M754 was mixed with 50 μM ATP in the presence of 0−50 μM ADP are shown in Figure 6. As in the experiment when ADP was premixed with acto•M754, the presence of ADP produces two phases. The amplitude of the fast phase decreased and the slow phase increased as ADP concentration was increased, and 50% of the amplitude

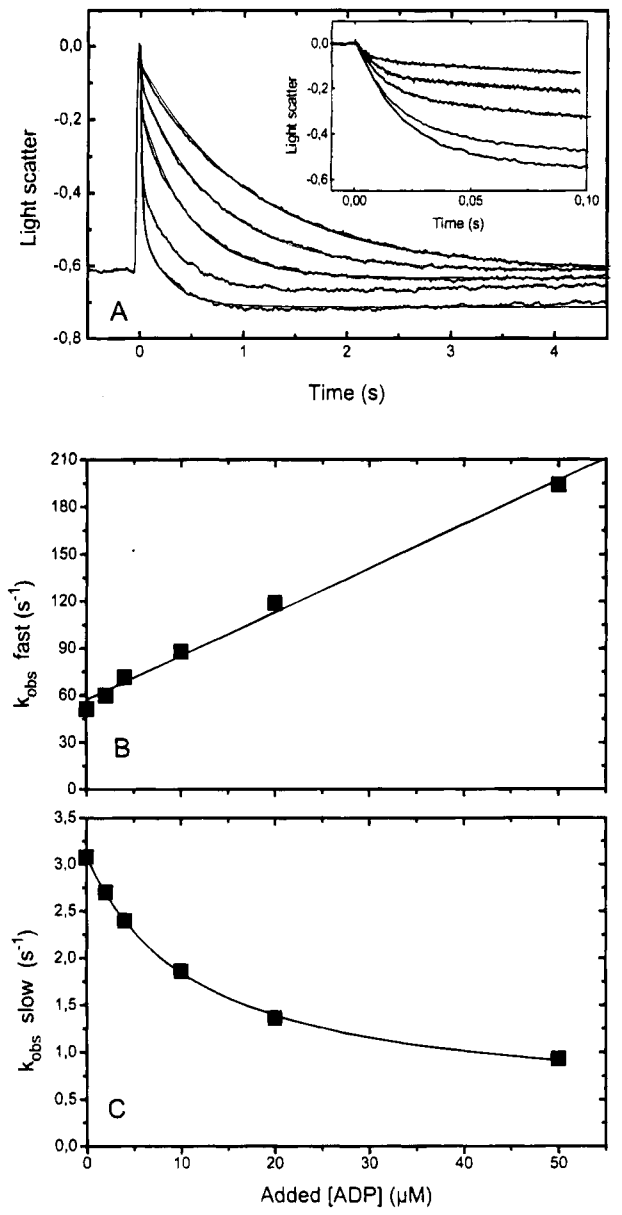

FIGURE 6: Competitive binding of ADP and ATP to acto•M754. (A) Light-scattering changes observed when 50 μM ATP, premixed with various concentration of ADP, is mixed with 0.25 μM acto•M754. The inset shows the same measurements made on a faster time scale. Added ADP concentrations: 0, 2, 10, 20, 50 μM. The best fits to one or two exponentials are shown superimposed, and the observed rate constants for the fast and slow phases are plotted in panels B and C, respectively. The data in panel B have been fitted to a straight line (slope = 2.9×10^6 M^{-1} s1$-^1$ and interpret 56 s^{-1}), and a smooth curve has been drawn through the data in panel C.

was fast phase at approximately 15 μM ADP. The observed rate constant of the slow phase decreased with increasing ADP concentration, and this reduction in k_{obs} is a measure of the efficiency with which the ADP that dissociates from acto•M754 is replaced by ATP. The k_{obs} was reduced by a factor of 2 at 15 μM ADP and suggests that 50% of the released ADP is replaced by ATP. Thus, analysis of both the amplitudes and the observed rate constant of the slow phase suggests that 15 μM ADP and 50 μM ATP bind to acto•M754 with equal rates; i.e., the second-order rate constant for ADP binding is approximately 3 times faster than that of ATP. This conclusion is supported by analysis of the observed rate constant of the fast phase which increases linearly with increasing [ADP]. For a model where both ADP binding and ATP binding are essentially irreversible on the time scale of the fast phase, k_{obs} (fast phase) = k_T[ATP] + k_D[ADP], where k_T and k_D are the apparent second-order rate constants of ATP and ADP binding, respectively. The slope of the fitted line gives a second-order rate constant of ADP binding of 2.8×10^6 M^{-1} s^{-1} compared to 1.5×10^6 M^{-1} s^{-1} for ATP (Figure 4).

The tight binding of ADP to acto•M754 raises the question as to the nature of the protein−ADP interaction in the acto•M754 complex. For acto•S1 and acto•MHF, ADP is bound in two ways: A small fraction is bound tightly as in the actin-free complex, and the majority is bound weakly (Geeves, 1989; Woodward et al., 1991; Geeves and Manstein, unpublished experiments). Thus, the tighter binding to M754 may reflect an increase in occupancy of the tightly bound form of ADP. The fluorescence of mantADP is enhanced when it binds to S1, MHF, or M754. The fluorescence of mantADP is also enhanced in the form tightly bound to acto•S1 or acto•MHF but not in the weakly bound form. We therefore measured the ATP-induced dissociation of acto•M754 which had been preincubated with a small excess of mantADP. The light-scattering signal was described by a double exponential with observed rate constants of 5 and 1 s^{-1}. The fast event corresponded to the major component of the signal. The observed rate constants were independent of ATP concentrations above 100 μM, and therefore the major process defines the rate constant of mantADP dissociation. Monitoring the same reaction using mant fluorescence shows no significant change in signal, indicating that the mantADP is displaced with little change in mant fluorescence as is observed for acto•S1 and acto•MHF.

DISCUSSION

In the absence of actin, M754 hydrolyzes ATP with a k_{cat} similar to that determined for MHF and rabbit S1, suggesting no major difference in the overall reaction. However, detailed transient kinetic analysis shows several major differences between M754 and the LCD-bearing myosin head fragment. The second-order rate constant for ATP binding to M754 is 16-fold slower than that observed for MHF, and 7-fold reductions in binding rate constants are also seen with mantATP and mantADP. Direct comparison to the rate of ADP binding to MHF is not possible, but it seems that nucleotides bind in general ~10 times slower to M754 than to MHF. Together, these data suggest that either access to the nucleotide site is more difficult, or recognition of free nucleotide is compromised, or the conformational change induced by nucleotide binding has a higher activation energy barrier. Once the nucleotide has bound, however, recognition of the nucleotide by M754 is much better. The rate constant of the ATP cleavage step is ~3 times faster, the dissociation rate constant for mantADP (k_{+5}) is ~100-fold reduced, and the affinity for ADP (K_5) is ~100-fold tighter.

M754 binds to actin with a similar affinity (K_D = 0.04 μM) as MHF (K_D = 0.07 μM), indicating that the truncation of the neck region causes only a slight peturbation in the part of the structure that forms the actin binding site. However, binding of M754 to actin seems to have a major effect on other parts of the structure and causes large changes in the affinity for nucleotides. The second-order rate constant for ATP binding is increased ~30-fold in the presence of

actin and is thus comparable to that of rabbit S1 and 10-fold faster than for acto•MHF (which compares with a ~20-fold lower rate of binding in the absence of actin). The rate constant for ADP binding is similarly increased 20-fold. These results suggest that the nucleotide site is not fully formed in M754 but binding to actin stabilizes the structure in general and the nucleotide binding site in particular.

Analysis of the rate of the ATP-induced dissociation of acto•M754 suggests that the initial binding of ATP (K_1) is no more than 5 times tighter than for MHF and the maximum rate constant of actin dissociation (controlled by k_{+2}, a conformational change of the acto•M754•ATP complex which results in stronger ATP binding and weaker actin binding) is at least double that of MHF. This suggests that the loss of the light chain binding domain has, in addition to perturbations around the nucleotide binding site, also affected the communication between the nucleotide and actin binding sites.

The perturbations of the nucleotide site and the communication between both sites are confirmed by the results on ADP binding to acto•M754. Actin binding causes a minor reduction in the affinity of M754 for ADP but accelerates ADP-release ~40-fold. The binding of ADP to M754, even in the presence of actin, is tight, and the affinity of ADP is 235-fold higher for acto•M754 than for acto•MHF. The nature of the bound ADP has changed between M754•ADP and acto•M754•ADP. This is reflected in the lack of a fluorescence change on displacing mantADP from acto•M754 compared to the large fluorescence change on displacement from M754 in the absence of actin.

The release of ADP from acto•M754 is slow enough for this to become limiting for the overall rate of ATP hydrolysis, and the k_{cat} for the ATPase should therefore be $\leq 2.3\ s^{-1}$. However, in agreement with the results described by Itakura and co-workers (Itakura et al., 1993), we observed a steady-state ATPase rate that continued to increase almost linearly up to the highest actin concentration measured. At 40 μM actin and 2 mM ATP, we observed a rate of $4.8\ s^{-1}$ for M754 which is 5-fold greater than the activity measured for MHF (Manstein et al., 1989). These findings can be accommodated by a model that introduces an additional acto•M754•ADP state that forms no part of the ATPase cycle. This additional state is only occupied in the absence of ATP or at ATP concentrations much smaller than those employed in the steady-state turnover experiments.

In contrast to the results obtained with the recombinant *D. discoideum* catalytic domains, a proteolytically prepared myosin motor domain from skeletal muscle that lacked the LCD displayed an actin-activated ATPase very similar to S1 (Waller et al., 1995). However, this discrepancy may be explained by differences in the exact location of the heavy chain truncation. Preliminary experiments with two slightly larger *D. discoideum* catalytic domain fragments show that the kinetic behavior of these proteins is indeed more similar to that of the light chain bearing fragment MHF (Geeves and Manstein, unpublished experiments).

In conclusion, M754 behaves in many general respects like other myosins or myosin fragments, but there are significant differences. The protein may be useful for site-directed mutagenic studies of myosin to map out the important structural features which are involved in actin binding, nucleotide binding, and ATP hydrolysis, but the major function as a motor seems to be significantly impaired by truncation of the heavy chain at or near isoleucine-754.

ACKNOWLEDGMENT

We thank D. M. Hunt, A. Becker, N. Adamek, and S. Kurzawa for their contributions to the work and Dr. J. F. Eccleston (NIMR, London) for his help and constructive discussions.

REFERENCES

Chang, A. C. M., Slade, M. B., & Williams, K. L. (1990) *Plasmid 24*, 208−217.
Criddle, A. H., Geeves, M. A., & Jeffries, T. A. (1985) *Biochem. J. 232*, 343−349.
De Lozanne, A., & Spudich, J. A. (1987) *Science 236*, 1086−1091.
Egelhoff, T. T., Titus, M. A., Manstein, D. J., Ruppel, K. M., & Spudich, J. A. (1991) *Methods Enzymol. 96*, 319−334.
Finer, J. T., Simmons, R. M., & Spudich, J. A. (1994) *Nature 368*, 113−119.
Fisher, A. J., Smith, C. A., Thoden, J., Smith, R., Sutoh, K., Holden, H. M., & Rayment, I. (1995a) *Biophys. J. 68*, 19s−28s.
Fisher, A. J., Smith, C. A., Thoden, J. B., Smith, R., Sutoh, K., Holden, H. M., & Rayment, I. (1995b) *Biochemistry 34*, 8960−8972.
Geeves, M. A. (1989) *Biochemistry 28*, 5864−5871.
Geeves, M. A., & Jeffries, T. A. (1988) *Biochem. J. 256*, 41−46.
Geeves, M. A., Goody, R. S., & Gutfreund, H. (1984) *J. Muscle Res. Cell Motil. 5*, 351−361.
Goldman, Y. E., Hibberd, M. G., McCray, J. A., & Trentham, D. R. (1982) *Nature 300*, 701−705.
Hiratsuka, T. (1983) *Biochim. Biophys. Acta 724*, 496−508.
Huxley, H. E., Simmons, R. M., Faruqi, A. R., Kress, M., Bordas, J., & Koch, M. H. J. (1983) *J. Mol. Biol. 169*, 469−506.
Itakura, S., Yamakawa, H., Toyoshima, Y. Y., Ishijima, A., Kojima, T., Harada, Y., Yanagida, T., Wakabayashi, T., & Sutoh, K. (1993) *Biochem. Biophys. Res. Commun. 196*, 1504−1510.
Kouyama, T., & Mihashi, K. (1981) *Eur. J. Biochem. 114*, 33−38.
Lehrer, S. S., & Kewar, G. (1972) *Biochemistry 11*, 1211−1217.
Leiting, B., Lindner, I. J., & Noegel, A. A. (1990) *Mol. Cell. Biol. 10*, 3727−3736.
Lombardi, V., Piazzesi, G., Ferenczi, M. A., Thirwell, H., Dobbie, I., & Irving, M. (1995) *Nature 374*, 553−555.
Lowey, S., Waller, G. S., & Trybus, K. M. (1993) *Nature 365*, 454−456.
Lymn, R. W., & Taylor, E. W. (1971) *Biochemistry 10*, 4617−4624.
Manstein, D. J., & Hunt, D. M. (1995) *J. Muscle Res. Cell Motil. 16*, 325−332.
Manstein, D. J., Ruppel, K. M., & Spudich, J. A. (1989) *Science 246*, 656−658.
Manstein, D. J., Schuster, H.-P., Morandini, P., & Hunt, D. M. (1995) *Gene 162*, 129−134.
Marston, S. B., & Taylor, E. W. (1980) *J. Mol. Biol. 139*, 573−600.
Millar, N. C., & Geeves, M. A. (1983) *FEBS Lett. 160*, 141−148.
Perrin, S., & Gilliland, G. (1990) *Nucleic Acids Res. 18*, 7433−7438.
Rayment, I., Holden, H.M., Whittaker, M., Yohn, C. B., Lorenz, M., Holmes, K. C., & Milligan, R. A. (1993a) *Science 261*, 58−65.
Rayment, I., Rypniewski, W. R., Schmidt-Bäse, K., Smith, R., Tomchick, D. R., Benning, M. M., Winkelmann, D. A., Wesenberg, G., & Holden, H. M. (1993b) *Science 261*, 50−58.
Ritchie, M. D., Geeves, M. A., Woodward, S. K. A., & Manstein, D. J. (1993) *Proc. Natl. Acad. Sci. U.S.A. 90*, 8619−8623.
Sambrook, J., Fritsch, E. F., & Maniatis, T. (1989) in *Molecular cloning: a laboratory* manual, Cold Spring Harbor Laboratory Press, Cold Spring Harbor, NY.
Schröder, R. R., Manstein, D. J., Jahn, W., Holden, H., Rayment, I., Holmes, K. C., & Spudich, J. A. (1993) *Nature 364*, 171−174.
Sellers, J. R. (1985) *J. Biol. Chem. 260*, 15815−15819.

Siemankowski, R. F., & White, H. D. (1984) *J. Biol. Chem. 259*, 5045−5053.
Slade, M. B., Chang, A. C. M., & Williams, K. L. (1990) *Plasmid 24*, 195−207.
Smith, C. A., & Rayment, I. (1995) *Biochemistry 34*, 8973−8981.
Taylor, E. W. (1979) *Crit. Rev. Biochem. 6*, 103−164.
Trentham, D. R., Eccleston, J. F., & Bagshaw, C. R. (1976) *Q. Rev. Biophys. 9*, 217−281.
Uyeda, T. Q. P., & Spudich, J. A. (1993) *Science 262*, 1867−1870.
Uyeda, T. Q. P., Warrick, H. M., Kron, S. J., & Spudich, J. A. (1991) *Nature 352*, 307−311.
Waller, G. S., Ouyang, G., Swafford, J., Vibert, P., & Lowey, S. (1995) *J. Biol. Chem. 270*, 15348−15352.
West, J. J., Nagy, B., & Gergely, J. (1967) *Biochem. Biophys. Res. Commun. 29*, 611−629.
White, H. D. (1982) *Methods Enzymol. 85*, 698−708.
Woodward, S. K. A., Eccleston, J. F., & Geeves, M. A. (1991) *Biochemistry 30*, 422−430.
Xie, X., Harrison, D. H., Schlichting, I., Sweet, R. M., Kalabokis, V. N., Szent-Gyorgyi, A. G., & Cohen, C. (1994) *Nature 368*, 306−312.
Yanisch-Perron, C., Vieira, J., & Messing, J. (1985) *Gene 33*, 103−119.

BI951570S